Gene 737 (2020) 144437

Contents lists available at ScienceDirect

Gene

journal homepage: www.elsevier.com/locate/gene

Functional expression of ZNF467 and PCBP2 supports adipogenic lineage commitment in adipose-derived mesenchymal stem cells

Martina Gluscevic[a], Christopher R. Paradise[b,c], Amel Dudakovic[a,d], Marcel Karperien[e], Allan B. Dietz[f], Andre J. van Wijnen[a,c,d,*], David R. Deyle[a,g,h,*]

[a] Department of Orthopedic Surgery, Mayo Clinic, Rochester, MN, United States
[b] Mayo Clinic Graduate School of Biomedical Sciences, Mayo Clinic, Rochester, MN, United States
[c] Center for Regenerative Medicine, Mayo Clinic, Rochester, MN, United States
[d] Department of Biochemistry and Molecular Biology, Mayo Clinic, Rochester, MN, United States
[e] Department of Developmental BioEngineering, University of Twente, Enschede, Netherlands
[f] Department of Laboratory Medicine and Pathology, Mayo Clinic, Rochester, MN, United States
[g] Department of Medical Genetics, Mayo Clinic, Rochester, MN, United States
[h] Department of Molecular Medicine, Mayo Clinic, Rochester, MN, United States

ARTICLE INFO

Keywords:
Adipose-derived mesenchymal stromal/stem cells
Adipogenic differentiation

ABSTRACT

Bone marrow-derived mesenchymal stromal/stem cells (BMSCs) have the potential to be employed in many different skeletal therapies. A major limitation to utilizing BMSCs as a therapeutic strategy in human disease and tissue regeneration is the low cell numbers obtained from initial isolation necessitating multiple cell passages that can lead to decreased cell quality. Adipose-derived mesenchymal stromal/stem cells (AMSCs) have been proposed as an alternative cell source for regenerative therapies; however the differentiation capacity of these cells differs from BMSCs. To understand the differences between BMSCs and AMSCs, we compared the global gene expression profiles of BMSCs and AMSCs and identified two genes, PCBP2 and ZNF467 that were differentially expressed between AMSCs and BMSCs. We demonstrate that PCBP2 and ZNF467 impact adipogenic but not osteogenic differentiation, further supporting evidence that AMSCs and BMSCs appear to be adapted to their microenvironment.

1. Introduction

Regenerative medicine is a translational branch of biomedical research that employs stem cells (SCs) and tissue engineering to treat chronic diseases and severe injuries with the goal to restore normal structure and function of damaged tissues and organs. The use of stem cells to treat bone, skin and corneal injuries has been proven to be safe (Gómez-Barrena, 2011; Rama, 2010; Badiavas and Falanga, 2003). Other conditions that have a potential to benefit from these approaches include hematologic malignancies, myocardial infarction, heart failure, and diabetes mellitus (Kim and Cho, 2013).

Mesenchymal stromal/stem cells (MSCs) are multipotent stem cells that have ability to differentiate into osteoblasts, chondrocytes, adipocytes, and myocytes (Pittenger, 1999; De Bari et al., 2001). They can be derived from multiple sources, including bone marrow, adipose tissue, dental pulp, amniotic membrane and fluid, peripheral blood, skin and synovial fluid (Mushahary et al., 2018). Although the wide array of MSCs are described as having similar multi-lineage differentiation capacity, a growing amount of evidence supports that they differ in stem cell properties and are uniquely programmed by the tissue microenvironment in which they reside(Mazini et al., 2019).

Bone marrow-derived stem cells (BMSCs) are the most extensively studied and frequently used type of stem cells to date. Because these cells reside in the bone marrow space and have a strong osteogenic potential, they are the ideal choice for treatment of bone defects and skeletal degenerative disorders such as osteoarthritis. However, their applicability to human disease has been constrained by inadequate cell numbers for transplantation due to the painful isolation procedure and their decreased abundance with age. To generate sufficient cell numbers, BMSCs need to be passaged multiple times, which exposes them to

Abbreviations: AMSCs, adipose-derived mesenchymal stromal/stem cells; BMSCs, bone marrow-derived mesenchymal stromal/stem cells; KLF, Krüppel-like family of transcription factors; PCBP, Poly(rC) binding protein; Poly(C), polycytosine

* Corresponding authors at: 200 First Street SW, Medical Sciences Building 3-81, Rochester, MN 55905, USA (D.R. Deyle); 200 First Street SW, Medical Sciences Building 3-69, Rochester, MN 55905, USA (A.J. van Wijnen).
E-mail addresses: vanwijnen.andre@mayo.edu (A.J. van Wijnen), deyle.david@mayo.edu (D.R. Deyle).

https://doi.org/10.1016/j.gene.2020.144437
Received 27 January 2020; Accepted 3 February 2020
Available online 04 February 2020
0378-1119/

Table 1
Primer sequences used in PCR reactions.

Gene name	Forward primer sequence	Reverse primer sequence
GAPDH	ATGTTCGTCATGGGTGTGAA	TGTGGTCATGAGTCCTTCCA
AKT1	ATGGCGCTGAGATTGTGTCA	CCCGGTACACCACGTTCTTC
ZNF467	GCCCCAGCATCTATCGTTACT	CTGGCTCCAGTTTGTACGC
PCBP3	AGCGCCATTGTGAGCAGA	GGGGAGGAAAGGGGGTTTG
ALPL	ACTGGTACTCAGACAACGAGAT	ACGTCAATGTCCCTGATGTTATG
BGLAP	GGCGCTACCTGTATCAATGG	GTGGTCAGCCAACTCGTCA
COL1A1	GTAACAGCGGTGAACCTGG	CCTCGCTTTCCTTCCTCTCC
TNFRSF11	GTGTGCGAATGCAAGGAAGG	CCACTCCAAATCCAGGAGGG
RUNX2	ATGTGTTTGTTTCAGCAGCA	TCCCTAAAGTCACTCGGTATGTGTA
ADIPOQ	AACATGCCCATTCGCTTTACC	TAGGCAAAGTAGTACAGCCCA
CEBPa	CGACATCAGCGCCTACAT	CCAGGAACTCGTCGTTGA
CEBPb	AACTCTCTGCTTCTCCCTCTG	AAGCCCGTAGGAACATCTTT
FABP4	GCAGAAATGGGATGGAAAATCA	ACGCATTCCACCACCAGTTTA
PPARγ	TGGAATTAGATGACAGCGACTTGG	CTGGAGCAGCTTGGCAAACA

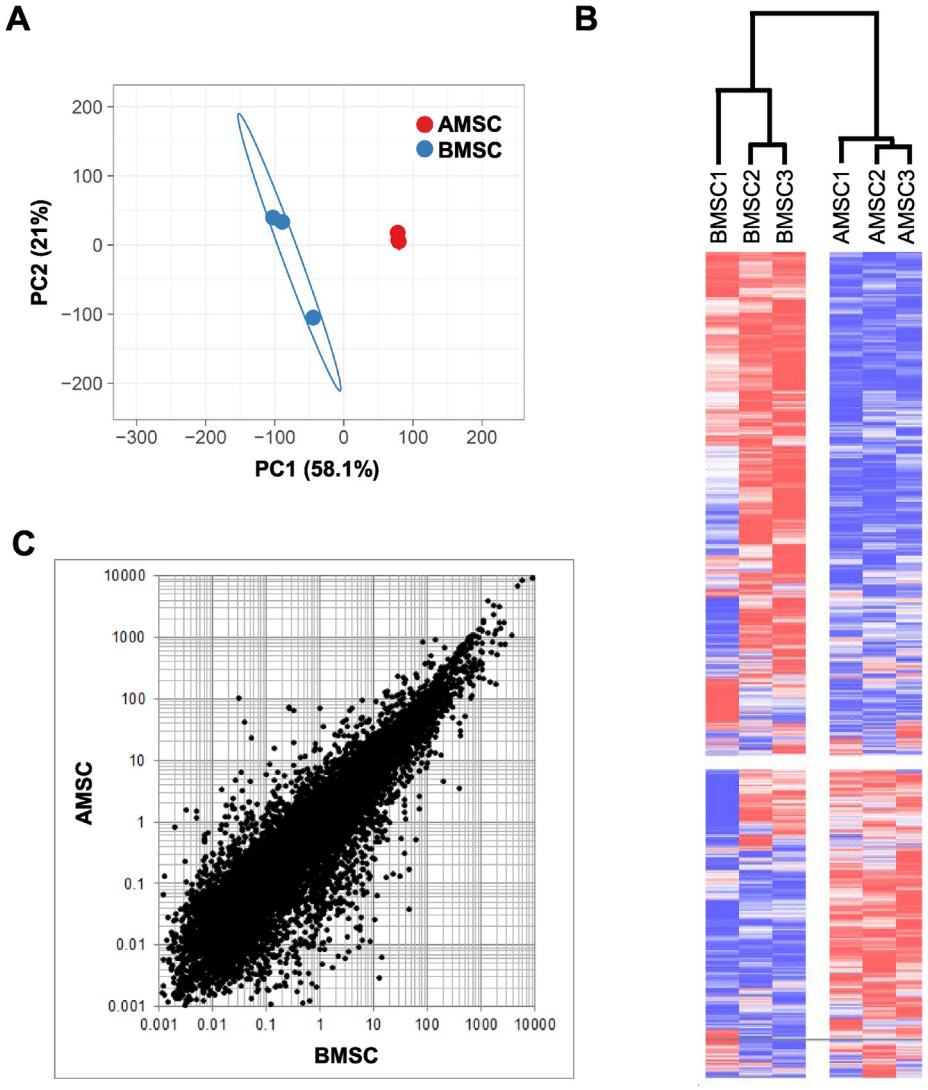

Fig. 1. Comparison of global RNA-seq expression patterns in AMSCs and BMSCs. Principle component analysis (A) (n = 3; overlay in AMSCs samples), heat map (B), global gene expression profile of AMSCs shown as scatter plot against BMSCs and (C) (n = 3) analysis of 13,445 expressed genes showed that the RNA samples from three AMSC lines were similar to three BMSC lines, but had unique differences.

potential contamination, oxidative stress, mutations, and senescence (Drela et al., 2019; Turinetto et al., 2016).

To circumvent this issue, alternative sources of MSCs have been explored to treat bone disorders, such as adipose-derived mesenchymal stem cells (AMSCs). AMSCs are a favorable alternative as they are easily isolated and yield a large number of cells after primary digests or brief cell culture. Unfortunately, it has proven more difficult to direct AMSCs towards the osteogenic lineage than BMSCs. Our group has previously evaluated in vitro differentiation, cell surface marker expression, in vivo safety and efficacy, and the transcriptome of clinical grade

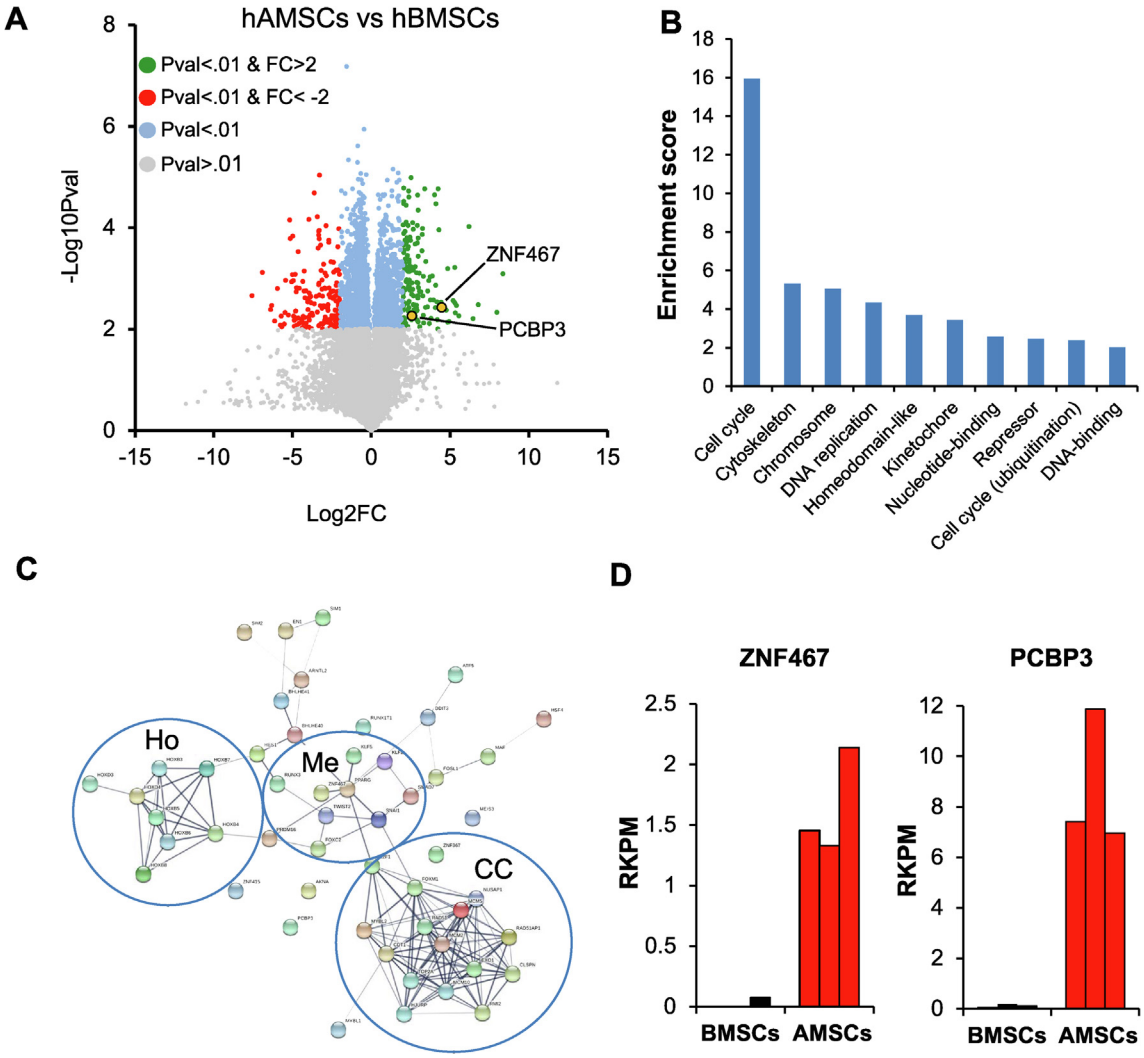

Fig. 2. Differentially expressed genes between AMSCs and BMSCs. (A) Comparative analysis of expression values in AMSCs vs BMSCs for genes with RPKM > 0.3 (n = 13,445) (B) The top 10 most enriched gene categories determined by gene ontology analysis from the up-or down-regulated genes in AMSCs vs BMSCs. (C) STRING analysis identified 3 major gene clusters, HOX genes (Ho), cell cycle/DNA replication genes (CC), and mesenchymal differentiation genes (Me) of differentially expressed genes. Five genes MEIS3, ZNF367, ZNF415, AKNA, and PCBP3 did not have links to other genes. (D) Expression of ZNF467 and PCBP3 in AMSCs and BMSCs shown in RPKM values (n = 3).

adipose-derived MSCs to characterize their cellular phenotype(Riester, 2017; Camilleri, 2016; Dudakovic, 2014; Dudakovic, 2015; Dudakovic, 2015; Lewallen, 2016; Dietz, 2017; Galeano-Garces, 2017). In this study, we compared AMSCs and BMSCs to help understand what makes them unique and which differences need to be overcome in order for AMSCs to be used for bone regeneration.

2. Materials and methods

2.1. Cell isolation and maintenance

Adipose-derived mesenchymal stromal cells (AMSCs) were isolated from lipo-aspirates obtained from consenting donors who underwent elective removal of subcutaneous adipose tissue with approval from the Mayo Clinic Institutional Review Board as previously described (Crespo-Diaz, 2011; Mader, 2013). Briefly, adipose tissue was enzymatically digested using 0.075% Type I collagenase (Worthington Biochemicals, Lakewood, NJ) for 1.5 h at 37 °C. Adipocytes were separated from the stromal vascular fraction by low speed centrifugation (5 min at 400 g) and the adipose supernatant was removed. The cell pellet was rinsed with PBS and passed through cell strainers: 70 μm followed by 40 μm (BD Biosciences, San Jose, CA). The resulting fraction of AMSCs was maintained in 175 cm^2 flasks at a cell density of 1–2.5 × 10^3 cells/cm^2 in Advanced MEM maintenance medium containing 5% PLTMax (a clinical grade commercial platelet lysate product [Mill Creek Life Sciences, Rochester, MN]), 2 mM Glutamax (L-glutamine [Invitrogen, Carlsbad, CA]), 2 U/mL heparin (hospital pharmacy) and antibiotics (100 U/mL penicillin and 100 g/mL streptomycin [Life Technologies, Carlsbad, CA]) as described previously(Crespo-Diaz, 2011).

Bone-marrow derived mesenchymal stromal cells (BMSCs) were isolated from bone marrow aspirate of consented patients with approval of the local ethical committee of the Medisch Spectrum Twente. BMSCs were isolated and expanded as previously described (Georgi, 2015).

3. mRNA isolation

At indicated time points, cells were lysed using TRI-Reagent (Zymo Research) and RNA was isolated using the Direct-zol RNA isolation kit (Zymo Research). Purified RNA was quantified and quality tested using a NanoDrop 2000 spectrophotometer (Thermo Fischer Scientific).

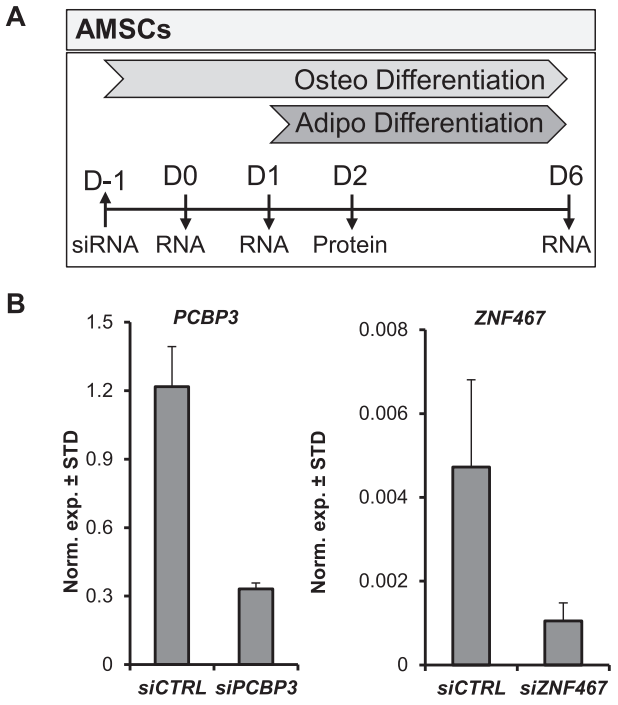

Fig. 3. Knockdown of PCBP3 and ZNF467 expression in AMSCs. (A) The experimental strategy to assess the role of PCBP3 and ZNF467 in osteogenic and adipogenic differentiation. (B) RT-qPCR validation of PCBP3 and ZNF467 knockdown after siRNA transfection (n = 3, ± standard deviation).

4. High throughput RNA-sequencing

AMSCs and BMSCs were plated at 10,000 cells/cm^2 and cultured in their respective standard culture conditions described above without differentiation cocktails. After one day, sub-confluent cells were lysed and mRNA isolated as described above. The resulting mRNA was utilized by the Mayo Clinic Sequencing core facility as described (Paradise, 2019).

RNA libraries were prepared according to the manufacturer's instructions for the TruSeq RNA Sample Prep Kit v2 (Illumina). Briefly, poly-A mRNA was purified from total RNA using oligo dT magnetic beads. Purified mRNA was fragmented at 95 °C for 8 min, eluted from the beads and primed for first strand cDNA synthesis. RNA fragments were copied into first strand cDNA using SuperScript III reverse transcriptase and random primers (Invitrogen). Next, second strand cDNA synthesis was performed using DNA polymerase I and RNase H. The double-stranded cDNA was purified using a single AMPure XP bead (Agencourt) clean-up step. The cDNA ends were repaired and phosphorylated using Klenow, T4 polymerase, and T4 polynucleotide kinase followed by a single AMPure XP bead clean-up. Blunt-ended cDNAs were modified to include a single 3′ adenylate (A) residue using Klenow exo- (3′ to 5′ exo minus). Paired-end DNA adaptors (Illumina) with a single "T" base overhang at the 3′ end were immediately ligated to the 'A tailed' cDNA population. Unique indexes, included in the standard TruSeq Kits (12-Set A and 12-Set B) were incorporated at the adaptor ligation step for multiplex sample loading on the flow cells. The resulting constructs were purified by two consecutive AMPure XP bead clean-up steps. The adapter-modified DNA fragments were enriched by 12 cycles of PCR using primers included in the Illumina Sample Prep Kit. The concentration and size distribution of the libraries was determined on an Agilent Bioanalyzer DNA 1000 chip. A final quantification, using Qubit fluorometry (Invitrogen), confirmed sample concentrations.

Libraries were loaded onto flow cells at concentrations of 8–10 pM to generate cluster densities of 700,000/mm^2 following the standard protocol for the Illumina cBot and cBot Paired end cluster kit version 3. Flow cells were sequenced as 51 × 2 paired end reads on an Illumina HiSeq 2000 using TruSeq SBS sequencing kit version 3 and HCS v2.0.12 data collection software. Base-calling was performed using Illumina's RTA version 1.17.21.3. The RNA-Seq data were analyzed using the standard RNA-Seq workflow by Mayo Bioinformatics Core called MAPRSeq v.1.2.1 (Kalari, 2014), which includes alignment with TopHat 2.0.6 (Kim, 2013) and quantification of gene expression using the HTSeq software (Anders et al., 2015). Normalized gene counts were also obtained from MAPRSeq where expression for each gene were normalized to 1 million reads and corrected for gene length (Reads Per Kilobase pair per Million mapped reads, RPKM).

5. Bioinformatic analysis

Genes with expression values > 0.3RPKM (n = 13,383) were utilized for subsequent analyses. Principal Component Analysis (PCA) was performed using ClustVis online tool (Metsalu and Vilo, 2015). Hierarchical clustering and heatmap analyses were conducted using the Morpheus matrix visualization online tool (Broad Institute, https://software.broadinstitute.org/morpheus). A Log2 adjustment was made for each gene row. Functional annotation clustering of differentially expressed genes was performed using DAVID Bioinformatics Resources 6.8 database (DAVID 6.8) (Shannon, 2003; Huang da et al., 2009). Protein-protein interaction networks were generated using STRING version 11 online tool (Szklarczyk, 2019).

6. Knockdown of ZNF467 and PCBP3 in AMSCs

AMSCs were plated in six-well plates (day −3) in maintenance medium at a cell density of 100,000 cells/well. Two days later (day −1) at 70% of cell confluence, siRNA transfections with control (D-001810-10-20, GE Healthcare, Little Chalfont, United Kingdom), PCBP3 (L-025367-01-0005, GE Healthcare, Little Chalfont, United Kingdom), and ZNF467 (L-013199-02-0005, GE Healthcare, Little Chalfont, United Kingdom) ON TARGETplus siRNA smartpools were performed using RNAiMAX as instructed by manufacturer (Invitrogen, Carlsbad, CA).

7. Osteogenic differentiation

AMSCs were plated in six-well plates and transfected with siRNAs against ZNF467 and PCBP3 as described above. Six hours after siRNA transfection osteogenic medium was added to opti-MEM medium in the same ratio with final concentrations 5% PLTMax, 50 μg/ml ascorbic acid, 10 mM β-glycerol phosphate, and 10 nM Dexamethasone. Media were changed and differentiation cocktail replenished every 2 days.

8. Adipogenic differentiation

AMSCs were plated in six-well plates (day -1) and transfected with siRNAs against ZNF467 and PCBP3 as described above. Two days after siRNA transfection (day 1) adipogenesis was induced by addition of adipogenic supplement (R&D Systems, Minneapolis, MN) to maintenance medium. Media were changed and differentiation cocktail replenished every 2 days.

9. mRNA quantitative real-time reverse transcriptase PCR (RT-qPCR)

mRNA was isolated using Direct-zol RNA isolation kit (Zymo Research) as described above. Isolated RNA was reverse transcribed into cDNA using SuperScript III First-Strand Synthesis System (Invitrogen, Carlsbad, CA). Gene expression was quantified using real-time PCR. Each qPCR reaction was performed with 10 ng cDNA per 10 μL, QuantiTect SYBR Green PCR Kit (Qiagen, Hilden, Germany) and the CFX384 real-time System machine (Bio-Rad, Hercules, CA).

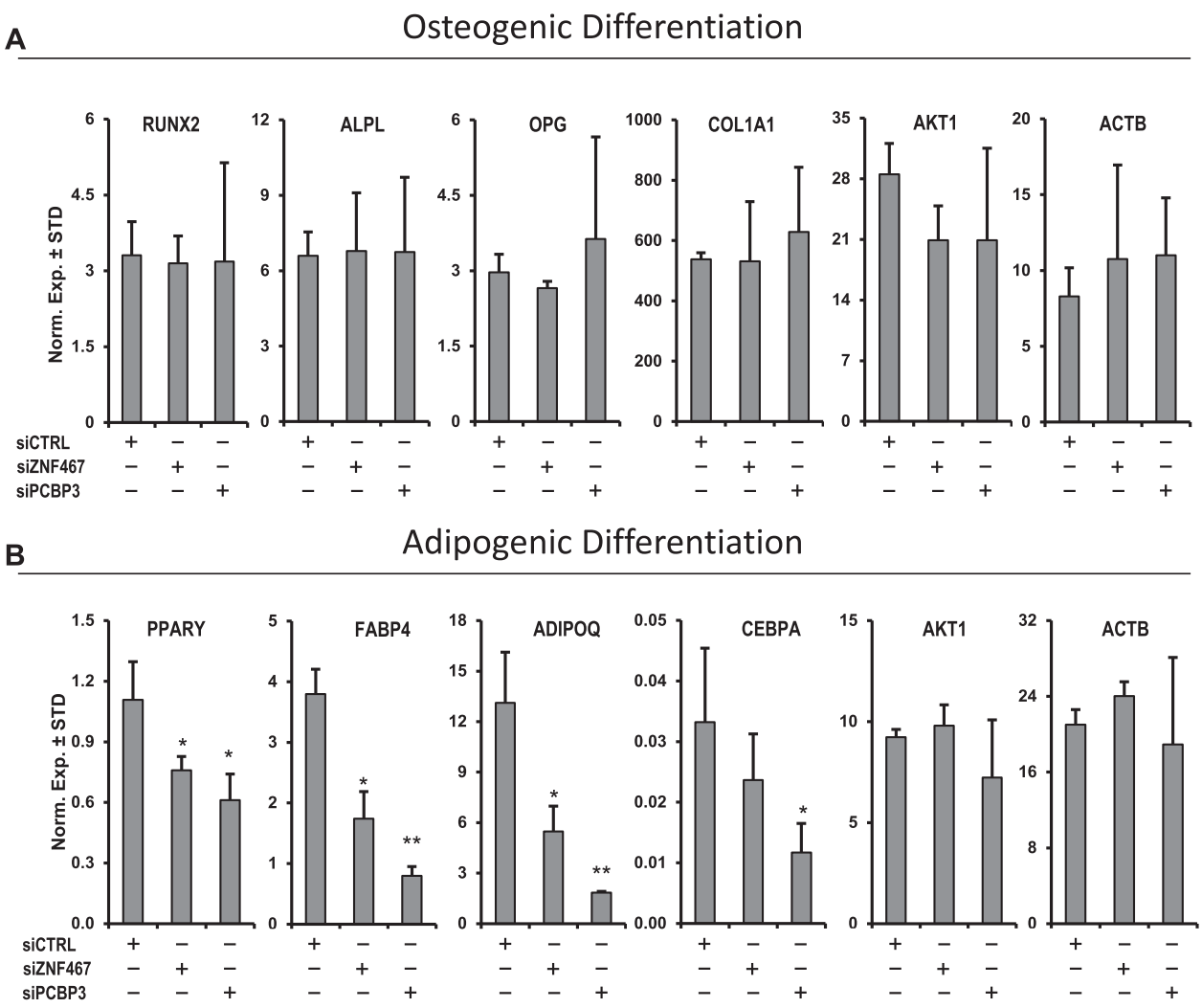

Fig. 4. The role of PCBP3 and ZNF467 in osteogenic and adipogenic differentiation. (A) PCBP3 or ZNF467 silencing analyzed by RT-qPCR in AMSCs grown in osteogenic conditions for expression levels of RUNX2, ALPL, OPG, and COL1A1 (n = 3, ± standard deviation). (B) PCBP3 or ZNF467 silencing analyzed by RT-qPCR in AMSCs grown under adipogenic conditions for expression levels of PPARγ, CEBPA, ADIPOQ, and FABP4 (n = 3, ± standard deviation). Housekeeping genes, AKT1 and ACTB, are shown as internal controls. (*P values < 0.05, **P values < 0.01).

Transcript levels were quantified using $2^{\Delta\Delta Ct}$ method and normalized to the housekeeping gene GAPDH (set at 100). Gene-specific primer sequences are shown in Table 1.

10. Results

To determine the cellular markers that may be unique to AMSCs, we performed gene expression profiling of AMSCs and BMSCs by RNA-seq. Our initial analysis of global gene expression profiles demonstrated that AMSCs and BMSCs exhibit differential expression profiles resulting in unique clustering of each cell types in a principal component analysis (Fig. 1A). These findings were confirmed by hierarchical clustering (Fig. 1B) as well as global gene expression distribution (Fig. 1C) of expressed genes.

Conservative filtering of mRNAs was performed by first selecting mRNAs expressed at robust levels (RPKM > 0.3). Within this gene set, transcripts with statistically significant (P < 0.01) differential gene expression (fold-change > 2.0) between samples were identified. Comparative analysis of RPKM values was performed on these robustly expressed genes revealing 163 significantly upregulated and 163 significantly downregulated genes in AMSCs compared to BMSCs (Fig. 2A). Table S1 shows the top 20 genes that exhibited maximal fold changes and were sorted for RPKMs primarily because fold change depends on background in non-expressing cells and therefore is arbitrary but RPKM is not. GO term analysis was performed and we found that the 326 up/down regulated genes were enriched for cell cycle, DNA replication, homeobox, and DNA binding pathways (Fig. 2B). Next, we performed STRING analysis to identify protein–protein interactions and found three specific clusters, HOX genes, cell cycle/DNA replication genes, and mesenchymal differentiation genes (Fig. 2C, Fig. S1). In addition, there were 5 genes that did not have any known interactions with other genes in this subset. The GO analysis of the top 20 from Table S1 revealed that six of the most robustly expressed proteins are either well-studied Hox proteins, which may represent vestiges of body patterning, or novel gene regulators in the nucleus that have remained underexplored. Of the different cellular pathways, we further examined the DNA binding genes because transcription factors that are upregulated in AMSCs could play a role in adipogenic differentiation. We chose to further analyze two transcription regulators PCBP3 and ZNF467 primarily as their function in AMSCs is not understood. Expression of both of these genes was significantly upregulated in AMSCs (Fig. 2D).

After identifying these two candidate genes, we functionally validated the role of ZNF467 and PCBP3 utilizing silencing RNA (siRNA) interference and assessing the impact on osteogenic and adipogenic differentiation of AMSCs (Fig. 3A). Gene expression analyses by qPCR

confirmed that ZNF467 and PCBP3 mRNA levels were depleted as expected (Fig. 3B). Osteogenic differentiation after silencing of ZNF467 or PCBP3 did not reduce the expression of bone-specific markers RUNX2, ALPL, OPG, or COL1A1 as assessed by RT-qPCR analysis (Fig. 4A). Conversely, AMSCs grown in adipogenic medium after ZNF467 or PCBP3 silencing demonstrated a significant reduction in adipocyte-specific markers PPARγ, CEBPA, ADIPOQ, and FABP4 (Fig. 4B). Taken together, these results indicate that while ZNF467 and PCBP3 expression does not have an impact on osteogenic differentiation, they do play a significant role in the development of adipocytes.

11. Discussion

MSCs are critically important for the normal development of different tissues and therapeutic potential in cellular regeneration. There is an increasing amount of evidence that stromal cells from different tissues diverge from their counterparts in differentiation potency and transcriptional profile which is reflective of their different developmental origin (Sacchetti, 2016). In our study we explored the gene expression profiles of BMSCs and AMSCs to identify genes that could provide a unique cellular signature for these cell types. Our study revealed two genes PCBP2 and ZNF467 that effect adipogenic differentiation of AMSCs.

PCBP3 encodes for poly(rC) binding protein (PCBP) 3 and is one of 5 known PCBPs (PCBP1-4 and hnRNP). These proteins are members of the KH-domain protein subfamily that bind to RNA with polycytosine [poly(C)] sequences (Makeyev and Liebhaber, 2000) in addition to single and double stranded C-rich DNA (Choi, 2009). The binding of poly(C) sequences by PCBPs results in a number of post-transcriptional regulations, including mRNA stabilization(Wang et al., 1995; Ho, 2013; Holcik and Liebhaber, 1997), translational silencing (Brown et al., 2016), translational enhancement (Shi, 2018), alternative splicing (Zhang, 2010; Ji et al., 2018) and regulation of gene expression (Ko and Loh, 2005; Thakur, 2003). Poly(rC) binding proteins were also shown to have ability to bind C-rich sequence of human telomeric DNA suggesting that they could have a role in regulation of telomere/telomerase functions(Du, 2005). While PCBP1, PCBP2, and hnRNP have been extensively studied, the exact function of PCBP3 is not completely understood. However, it has recently been shown that PCBP3 can bind both single and double-stranded poly(C) sequences and may act as a transcriptional repressor (Kang, 2012).

The function of ZFP467 in human cells has not yet been fully elucidated. In the mouse, it was isolated from hematogenic endothelial LO cells as an OSM-inducible mRNA (Nakayama et al., 2002). The mouse ortholog of Zfp467 belongs to the Krüppel-like family of transcription factors (KLF) consisting of 12 repeats of C2H2-type zinc finger motifs (Nakayama et al., 2002). Zfp467 is expressed ubiquitously and is thought to play a role in general cellular function (Nakayama et al., 2002). In addition, it has been shown to regulate osteoblast and adipocyte commitment. Overexpression of Zfp467 lead to delayed osteoblast differentiation and accelerated adipocytes differentiation (Quach, 2011), while suppression of Zfp467 promoted osteoblast differentiation (You, 2012). A more recent study indicated that Zfp467 may regulate Wnt signaling by promoting Sost binding to LRP5/6 (You et al., 2015).

AMSCs have been studied as a potential source of cells for skeletal repair; however, there is increasing evidence that AMSCs and BMSCs have unique biological differences. AMSCs are not as osteogenic as BMSCs and our data shows that there are significant differences between their gene expression profiles. We identified two transcription regulators that are highly expressed in AMSCs that support adipogenesis but have no effect on osteogenic differentiation. These results support the growing evidence that AMSCs and BMSCs are uniquely adapted to their microenvironment and have differential predispositions for lineage commitment and regeneration of specific tissues.

Declaration of Competing Interest

The authors declare that they have no known competing financial interests or personal relationships that could have appeared to influence the work reported in this paper.

Appendix A. Supplementary data

Supplementary data to this article can be found online at https://doi.org/10.1016/j.gene.2020.144437.

References

Gómez-Barrena, E., et al., 2011. Bone regeneration: stem cell therapies and clinical studies in orthopaedics and traumatology. J. Cell Mol. Med. 15, 1266–1286. https://doi.org/10.1111/j.1582-4934.2011.01265.x.

Rama, P., et al., 2010. Limbal stem-cell therapy and long-term corneal regeneration. N. Engl. J. Med. 363, 147–155. https://doi.org/10.1056/NEJMoa0905955.

Badiavas, E.V., Falanga, V., 2003. Treatment of chronic wounds with bone marrow–-derived cells. Arch. Dermatol. 139, 510–516. https://doi.org/10.1001/archderm.139.4.510.

Kim, N., Cho, S.G., 2013. Clinical applications of mesenchymal stem cells. Korean J. Intern. Med. 28, 387–402. https://doi.org/10.3904/kjim.2013.28.4.387.

Pittenger, M.F., et al., 1999. Multilineage potential of adult human mesenchymal stem cells. Science 284, 143–147. https://doi.org/10.1126/science.284.5411.143.

De Bari, C., Dell'Accio, F., Tylzanowski, P., Luyten, F.P., 2001. Multipotent mesenchymal stem cells from adult human synovial membrane. Arthritis Rheum. 44, 1928–1942. https://doi.org/10.1002/1529-0131(200108)44:8<1928::AID-ART331>3.0.CO;2-P.

Mushahary, D., Spittler, A., Kasper, C., Weber, V., Charwat, V., 2018. Isolation, cultivation, and characterization of human mesenchymal stem cells. Cytometry A 93, 19–31. https://doi.org/10.1002/cyto.a.23242.

Mazini, L., Rochette, L., Amine, M., Malka, G., 2019. Regenerative capacity of adipose derived stem cells (ADSCs), comparison with mesenchymal stem cells (MSCs). Int. J. Mol. Sci. 20. https://doi.org/10.3390/ijms20102523.

Drela, K., Stanaszek, L., Nowakowski, A., Kuczynska, Z., Lukomska, B., 2019. Experimental strategies of mesenchymal stem cell propagation: adverse events and potential risk of functional changes. Stem Cells Inter. 2019, 10. https://doi.org/10.1155/2019/7012692.

Turinetto, V., Vitale, E., Giachino, C., 2016. Senescence in human mesenchymal stem cells: functional changes and implications in stem cell-based therapy. Int. J. Mol. Sci. 17. https://doi.org/10.3390/ijms17071164.

Riester, S.M., et al., 2017. Safety studies for use of adipose tissue-derived mesenchymal stromal/stem cells in a rabbit model for osteoarthritis to support a phase I clinical trial. Stem Cells Transl. Med. 6, 910–922. https://doi.org/10.5966/sctm.2016-0097.

Camilleri, E.T., et al., 2016. Identification and validation of multiple cell surface markers of clinical-grade adipose-derived mesenchymal stromal cells as novel release criteria for good manufacturing practice-compliant production. Stem Cell Res. Ther. 7, 107. https://doi.org/10.1186/s13287-016-0370-8.

Dudakovic, A., et al., 2014. High-resolution molecular validation of self-renewal and spontaneous differentiation in clinical-grade adipose-tissue derived human mesenchymal stem cells. J. Cell. Biochem. 115, 1816–1828. https://doi.org/10.1002/jcb.24852.

Dudakovic, A., et al., 2015. Histone deacetylase inhibition destabilizes the multi-potent state of uncommitted adipose-derived mesenchymal stromal cells. J. Cell. Physiol. 230, 52–62. https://doi.org/10.1002/jcp.24680.

Dudakovic, A., et al., 2015. Epigenetic control of skeletal development by the histone methyltransferase Ezh2. J. Biol. Chem. 290, 27604–27617. https://doi.org/10.1074/jbc.M115.672345.

Lewallen, E.A., et al., 2016. Osteogenic potential of human adipose-tissue-derived mesenchymal stromal cells cultured on 3D-printed porous structured titanium. Gene 581, 95–106. https://doi.org/10.1016/j.gene.2016.01.015.

Dietz, A.B., et al., 2017. Autologous mesenchymal stem cells, applied in a bioabsorbable matrix, for treatment of perianal fistulas in patients with Crohn's disease. Gastroenterology 153, 59–62. https://doi.org/10.1053/j.gastro.2017.04.001. 59-62 e52.

Galeano-Garces, C., et al., 2017. Molecular validation of chondrogenic differentiation and hypoxia responsiveness of platelet-lysate expanded adipose tissue-derived human mesenchymal stromal cells. Cartilage 8, 283–299. https://doi.org/10.1177/1947603516659344.

Crespo-Diaz, R., et al., 2011. Platelet lysate consisting of a natural repair proteome supports human mesenchymal stem cell proliferation and chromosomal stability. Cell Transplant. 20, 797–812. https://doi.org/10.3727/096368910X543376.

Mader, E.K., et al., 2013. Optimizing patient derived mesenchymal stem cells as virus carriers for a phase I clinical trial in ovarian cancer. J. Transl. Med. 11, 20. https://doi.org/10.1186/1479-5876-11-20.

Georgi, N., et al., 2015. Differentiation of mesenchymal stem cells under hypoxia and normoxia: lipid profiles revealed by time-of-flight secondary ion mass spectrometry and multivariate analysis. Anal. Chem. 87, 3981–3988. https://doi.org/10.1021/acs.analchem.5b00114.

Paradise, C.R., et al., 2019. The epigenetic reader Brd4 is required for osteoblast differentiation. J. Cell. Physiol. https://doi.org/10.1002/jcp.29415.

Kalari, K.R., et al., 2014. MAP-RSeq: Mayo analysis pipeline for RNA sequencing. BMC Bioinf. 15, 224. https://doi.org/10.1186/1471-2105-15-224.
Kim, D., et al., 2013. TopHat2: accurate alignment of transcriptomes in the presence of insertions, deletions and gene fusions. Genome Biol. 14, R36. https://doi.org/10.1186/gb-2013-14-4-r36.
Anders, S., Pyl, P.T., Huber, W., 2015. HTSeq–a Python framework to work with high-throughput sequencing data. Bioinformatics 31, 166–169. https://doi.org/10.1093/bioinformatics/btu638.
Metsalu, T., Vilo, J., 2015. ClustVis: a web tool for visualizing clustering of multivariate data using Principal Component Analysis and heatmap. Nucleic Acids Res. 43, W566–W570. https://doi.org/10.1093/nar/gkv468.
Shannon, P., et al., 2003. Cytoscape: a software environment for integrated models of biomolecular interaction networks. Genome Res. 13, 2498–2504. https://doi.org/10.1101/gr.1239303.
Huang da, W., Sherman, B.T., Lempicki, R.A., 2009. Systematic and integrative analysis of large gene lists using DAVID bioinformatics resources. Nat. Protoc. 4, 44–57. https://doi.org/10.1038/nprot.2008.211.
Szklarczyk, D., et al., 2019. STRING v11: protein-protein association networks with increased coverage, supporting functional discovery in genome-wide experimental datasets. Nucleic Acids Res. 47, D607–D613. https://doi.org/10.1093/nar/gky1131.
Sacchetti, B., et al., 2016. No identical "Mesenchymal Stem Cells" at different times and sites: human committed progenitors of distinct origin and differentiation potential are incorporated as adventitial cells in microvessels. Stem Cell Rep. 6, 897–913. https://doi.org/10.1016/j.stemcr.2016.05.011.
Makeyev, A.V., Liebhaber, S.A., 2000. Identification of two novel mammalian genes establishes a subfamily of KH-domain RNA-binding proteins. Genomics 67, 301–316. https://doi.org/10.1006/geno.2000.6244.
Choi, H.S., et al., 2009. Poly(C)-binding proteins as transcriptional regulators of gene expression. Biochem. Biophys. Res. Commun. 380, 431–436. https://doi.org/10.1016/j.bbrc.2009.01.136.
Wang, X., Kiledjian, M., Weiss, I.M., Liebhaber, S.A., 1995. Detection and characterization of a 3' untranslated region ribonucleoprotein complex associated with human alpha-globin mRNA stability. Mol. Cell. Biol. 15, 1769–1777. https://doi.org/10.1128/mcb.15.3.1769.
Ho, J.J., et al., 2013. Active stabilization of human endothelial nitric oxide synthase mRNA by hnRNP E1 protects against antisense RNA and microRNAs. Mol. Cell. Biol. 33, 2029–2046. https://doi.org/10.1128/MCB.01257-12.
Holcik, M., Liebhaber, S.A., 1997. Four highly stable eukaryotic mRNAs assemble 3' untranslated region RNA-protein complexes sharing cis and trans components. Proc. Natl. Acad. Sci. USA 94, 2410–2414. https://doi.org/10.1073/pnas.94.6.2410.
Brown, A.S., Mohanty, B.K., Howe, P.H., 2016. Identification and characterization of an hnRNP E1 translational silencing motif. Nucleic Acids Res. 44, 5892–5907. https://doi.org/10.1093/nar/gkw241.
Shi, H., et al., 2018. PCBP1 depletion promotes tumorigenesis through attenuation of p27(Kip1) mRNA stability and translation. J. Exp. Clin. Cancer Res. 37, 187. https://doi.org/10.1186/s13046-018-0840-1.
Zhang, T., et al., 2010. PCBP-1 regulates alternative splicing of the CD44 gene and inhibits invasion in human hepatoma cell line HepG2 cells. Mol. Cancer 9, 72. https://doi.org/10.1186/1476-4598-9-72.
Ji, X., Humenik, J., Yang, D., Liebhaber, S.A., 2018. PolyC-binding proteins enhance expression of the CDK2 cell cycle regulatory protein via alternative splicing. Nucleic Acids Res. 46, 2030–2044. https://doi.org/10.1093/nar/gkx1255.
Ko, J.L., Loh, H.H., 2005. Poly C binding protein, a single-stranded DNA binding protein, regulates mouse mu-opioid receptor gene expression. J. Neurochem. 93, 749–761. https://doi.org/10.1111/j.1471-4159.2005.03089.x.
Thakur, S., et al., 2003. Regulation of BRCA1 transcription by specific single-stranded DNA binding factors. Mol. Cell. Biol. 23, 3774–3787. https://doi.org/10.1128/mcb.23.11.3774-3787.2003.
Du, Z., et al., 2005. Crystal structure of the first KH domain of human poly(C)-binding protein-2 in complex with a C-rich strand of human telomeric DNA at 1.7 A. J. Biol. Chem. 280, 38823–38830. https://doi.org/10.1074/jbc.M508183200.
Kang, D.-H., et al., 2012. Novel dual-binding function of a poly (C)-binding protein 3, transcriptional factor which binds the double-strand and single-stranded DNA sequence. Gene 501, 33–38. https://doi.org/10.1016/j.gene.2012.04.001.
Nakayama, K., Kim, K.W., Miyajima, A., 2002. A novel nuclear zinc finger protein EZI enhances nuclear retention and transactivation of STAT3. EMBO J. 21, 6174–6184. https://doi.org/10.1093/emboj/cdf596.
Quach, J.M., et al., 2011. Zinc finger protein 467 is a novel regulator of osteoblast and adipocyte commitment. J. Biol. Chem. 286, 4186–4198. https://doi.org/10.1074/jbc.M110.178251.
You, L., et al., 2012. Suppression of zinc finger protein 467 alleviates osteoporosis through promoting differentiation of adipose derived stem cells to osteoblasts. J. Transl. Med. 10, 11. https://doi.org/10.1186/1479-5876-10-11.
You, L., Chen, L., Pan, L., Gu, W.-S., Chen, J.-Y., 2015. Zinc finger protein 467 regulates Wnt signaling by modulating the expression of sclerostin in adipose derived stem cells. Biochem. Biophys. Res. Commun. 456, 598–604. https://doi.org/10.1016/j.bbrc.2014.11.120.